Biomechanics of the Mandible: Part II. Development of a 3-Dimensional Finite Element Model to Study Mandibular Functional Deformation in Subjects Treated with Dental Implants

Jehad Al-Sukhun, PhD, MSc, BDS[1]/John Kelleway[2]

Purpose: *The purpose of the study was to develop a finite element model of the human mandible and to compare the functional deformation predicted by the model with that detected clinically.* ***Materials and Methods:*** *Three patterns of mandibular deformation (medial convergence, corporal rotation and dorso-ventral shear) were studied clinically in 12 subjects using custom-fabricated displacement transducers mounted on endosseous implants in the premolar region. The mandibular arches of 12 patients with dental implants were modeled using finite element techniques based on computerized tomographic (CT) scan images of the jaw.* ***Results:*** *The finite element model was found to closely replicate the patterns of observed mandibular deformation. Differences between the predicted and measured deformation values were expressed as a percentage of the measured value and ranged between 0.0% and 22.2%. Medial convergence ranged between 14.4 and 58.4 μm. Dorso-ventral shear and corporal rotation ranged between 0.4 and 2.7 degrees.* ***Conclusions:*** *Using the finite element model described in this study, which represents the living human mandible, and clinical testing, there was close agreement between the predicted and measured deformation values. This study provided a high level of confidence in the finite element model and its ability to provide better insight into understanding the complex phenomena of functional mandibular deformation.* (More than 50 references.) INT J ORAL MAXILLOFAC IMPLANTS 2007;22:455–466

Key words: *finite element analysis, jaw deformation, stress*

The mandible is a specialized structure, where muscles, joints, and teeth work in a complex synergy. Function and form of the mandible are adapted to work in the highly developed masticatory system. The first concept of a junction between biomechanics and morphology was shown by Wolff[1] and described as functional adaptation of bony tissue. Further investigations by Frost[2] demonstrated the relationship between the amount of strain in the bony microenvironment and the subsequent biologic reaction.

The morphology of a bone is influenced by its mechanical environment and loading history.[1,2] This also applies to the mandible, and several researchers have suggested that the adaptive response of the primate mandibular symphysis to mechanical stress is reflected in its morphology.[3–6] In 1984, Hylander[6] postulated that at least three patterns of stress and deformation occurred in the primate symphysis. These are corporal rotation, symphyseal dorso-ventral shear, and medial convergence (Fig 1). *Corporal rotation (CR)* is the relative outward rotation of the 2 halves of the mandible as the corpora rotated and their coronal ends became farther apart relative to their apices. *Medial convergence (MC)* is the change in mandibular width during function. *Dorso-ventral (DV) shear* is the movement of the 2 halves of the mandible relative to one another in the vertical plane.

[1]Consultant, Oral and Maxillofacial Surgeon, Department of Oral and Maxillofacial Surgery, Sheikh Khalifeh Medical City, United Arab Emirates; Director, Euro-Oral Hammaslääkärikeskus, Helsinki, Finland.
[2]Senior Research Instructor, Eastman Dental Institute for Oral Health Care Sciences, University of London, United Kingdom.

Correspondence to: Dr Jehad Al-Sukhun, Department of Oral and Maxillofacial Surgery, Helsinki University Central Hospital, Kasarmikatu 11-13, PO Box 263, 00029 HUS, Helsinki, Finland. Fax: +3589483720. E-mail: Jalsukhun@hotmail.com, Jehad.Al-Sukhun@hus.fi

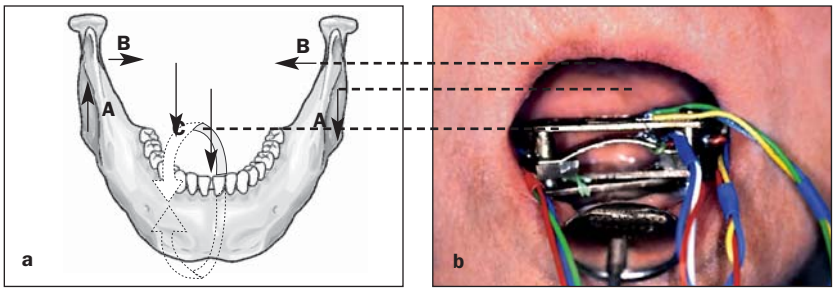

Fig 1 *(a)* Jaw deformation: A = medial convergence, B = corporal rotation, and C = dorso-ventral shear. *(b)* Frontal view of the oral cavity of a subject with strain-gauge transducers, mounted on 2 implants. The top horizontal, transverse beam was mounted to determine corporal rotation. The semicircular bridge beam was used next to determine medial convergence. At the bottom, the 2 crossed beams were mounted onto the 2 implants to determine dorso-ventral shear. The recorded strain data at the free end of each beam were then converted via calibration charts into microns and consequently expressed for the effect of jaw deformation in the case of medial convergence. In case of corporal rotation and dorso-ventral shear, the deflection of the free end of the beam was converted into angles, and deformation was expressed in degrees.

These patterns may influence the construction and performance of intraoral prostheses, especially implant-stabilized prostheses, which are linked to the jaw with relatively rigid interfaces. Although mandibular implant treatment has a high success rate, the long-term clinical significance of mandibular deformation on implant treatment is still unknown. The possibility that jaw deformation and the resulting stresses may be a source of implant failure, or enhance osseointegration, cannot be excluded.

Insights into mandibular deformation have been gained from measurements of regional surface strain in living macaques.[6,7–11] The extent to which these observations can be extrapolated to human beings is uncertain because of the distinct differences in morphology and function between the species. Currently, the direct measurement of bone strain using electrical strain gauges in living human subjects is impractical. Photoelastic measurements have also been made on physical models of the mandible,[12–14] but this technique is of limited quantitative value. As in the majority of experimental stress methods, its main disadvantage is that it is not appropriate for analyzing strain under in vivo conditions. However, the method is nondestructive and enables the investigator to visualize the distribution of surface strains. The most common approach has been to use mathematical modeling to specify the locations and orientations of putative muscle tension vectors 3-dimensionally. In these models, it has been assumed that the bone is a rigid structure, and as such behaves according to static equilibrium theory.[7,15,16] Mathematical models necessarily assume structural rigidity and concentricity in the sagittal view, factors which limit their usefulness. As an alternative, indirect mathematical approach, the finite element modeling technique enables the modeling of structures with intricate shapes and can be used to indirectly quantify their complex mechanical behavior at any theoretical point.[17] Since the finite element method uses the theories of elasticity and static equilibrium, the effects of multiple external forces acting on a system can be assessed as physical events in terms of deformations, stresses, or strains.

The purpose of this study was to develop a finite element model of the human mandible and to compare the functional deformation predicted by the model with that detected clinically.

MATERIALS AND METHODS

Clinical Study

The design of the clinical study was described in previous work but will be summarized here.[5,18] The subjects were 12 women between 47 and 65 years old. None of the subjects suffered from any temporomandibular joint dysfunction or systemic disease, and none was using any medication which might have adversely affected neuromuscular activity. Similarly, none was known to be suffering from any abnormality of bone metabolism. Measurements were made during a routine review visit. The subjects gave their informed consent, and the project was approved by a local ethics committee.

Each patient had 2 Nobel Biocare endosseous implants (diameter 3.75 mm; Nobel Biocare, Göteborg, Sweden) placed in the left and right mandibular premolar regions (1 implant per hemimandible). The 2 implants were placed vertically to the lower border of the mandible and equidistant from the median sagittal plane. The implants had been present for a minimum of 24 months and met recognized criteria of success.[5,18]

Three sets of displacement transducers were used to measure MC, CR, and DV shear. The convention and the design of the transducers were previously described.[5,18] The transducers were designed to fit to the transmucosal abutments (Fig 1). All strain-gauge beams were connected to Wheatstone bridge circuits in half-bridge designs, through a multichannel amplifier and an A/D converter (Microlink 3000, Bio Data, Manchester, UK) which provided the energizing voltage and signal conditioning circuitry. Data were processed through the multiplexed A/D converter linked via an IEEE 488 interface to a computer (486 SX; Tandon, Pallekelle, Sri Lanka). Processing was done using manufacturer-supplied software. Each patient was instructed to perform the following exercises 5 times in succession: *(1)* maximum opening of the mouth, followed by closing; *(2)* lateral excursions to the left and right sides; and *(3)* protrusion of the jaw. The recorded strain data at the free end of each beam was then converted via calibration charts into micrometers and consequently expressed for the effect of jaw deformation in the case of MC. In case of CR and DV shear, the deflection of the free end of the beam was converted into degrees, and deformation was expressed as an angular measurement.[17,18]

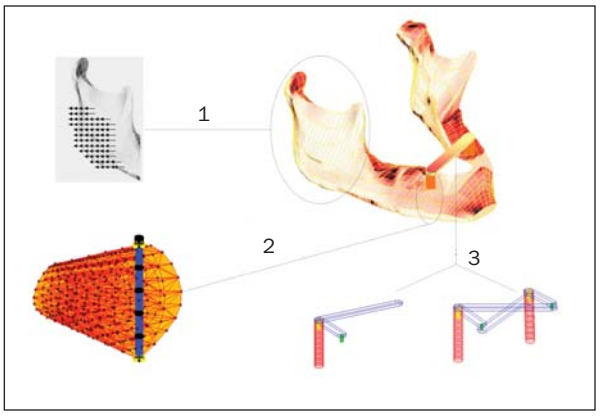

Fig 2 Anterolateral view of the modeled jaw with the 2 implants and the horizontal transverse beam in place. *(1)* Groups of parallel vectors simulating the masseter muscle were modeled as being directly attached to bone. *(2)* Finite element mesh for a bone cross section with implant *(black)* and abutment *(blue)* in place. Rigid fixation *(yellow)* was applied at the implant-bone interface. *(3)* The modeled beams *(blue)* mounted onto the implants *(red)* with a fastening cylinder *(yellow)*. The 2 crossed beams were used to predict DV shear. The transverse horizontal beam was used to predict CR.

Finite Element Study

Building a finite element model can be divided into 2 stages—geometric modeling and finite element modeling.

Geometric Modeling and Material Properties. The purpose of the geometric modeling stage is to represent geometry in terms of points (grids), lines, surfaces (patches), and volumes (hyper-patches). The geometry of the mandible of each patient was constructed based on computerized tomographic (CT) scans. Computerized tomography was performed using a Siemens Somatom CR CT scanner (Siemens, Erlangen, Germany). Voltage was 125 kV, MAS 500. Sagittal and coronal slices perpendicular to the inferior border of the mandible were obtained. The slices were 2 mm thick, with a 0.2-mm gap between slices.

The material properties of the finite element model of the mandibular bone was based on the measured x-ray attenuation coefficients. These coefficients (Hounsfield values) were directly converted into density values and then into elastic stiffness values on the basis of data reported by Carter and Hayes.[19] The derived bone properties were patient-specific (ie, based on the individual CT of each patient).

Finite Element Modeling. The geometric entities created in the previous step were mapped with finite elements and nodes. The complete geometry is now defined as a mesh of discrete pieces called elements, which are connected together at a finite number of points called nodes (Fig 2). The mapping was performed with the semiautomatic option (finite element generation [FEG]) available in Display III (NISA; EMRC, Troy, MI). The mesh volumes were subdivided into brick-shaped (6-sided with 24 degrees of freedom) and wedge-shaped (5-sided with 18 degrees of freedom) solid linear elements. The finite element model was checked for node coincidence and discontinuities (ie, gaps between elements).

Force analysis for any simulated mandibular movement requires the establishment of the contribution of each muscle to the overall forces of the system. These individual forces were determined along each muscle-specific line of pull according to 2 assumptions. First, large muscles are capable of producing more isometric contraction force than small ones, the tension in each muscle being proportional to the product of its physiological cross section and an assumed force constant per unit of cross-sectional area.[17,20,21] Second, various static mandibular movements involve different amounts of activation in a given muscle depending on the phase of the movement.[17] In other words, the same muscle may exhibit 100% activity during one movement and only 50% during another.

Thus, the resultant vector of muscle force (M_{ir}) for a particular muscle in isometric contraction during a specific movement could be given by the product

$$[X_{mi} \bullet K] \times EMG_{mi} = M_{ir}$$

Table 1a Number and Magnitudes of Muscle Loads Used in the Finite Element Model: Lateral Excursion

Muscle group	Muscle group cross section (cm^2)	Muscle weighting factor (N)	Nodes		Muscle orthogonal components											
					Right lateral excursion						Left lateral excursion					
					Right			Left			Right			Left		
			Right	Left	x	y	z	x	y	z	x	y	z	x	y	z
Superior masseter	2.38	190.4	50	50	−0.06	0.23	0.11	−0.22	0.94	0.45	−0.27	1.01	0.48	−0.04	0.17	0.08
Deep masseter	1.02	81.6	39	38	−0.07	0.10	−0.04	−0.24	0.33	−0.15	−0.29	0.40	−0.19	0.08	0.11	−0.05
Medial pterygoid	1.9	174.8	42	44	0.12	0.18	0.09	1.48	2.42	1.14	1.66	2.58	1.27	0.15	0.25	0.12
Ant. temporalis	2.4	158.0	20	20	−2.01	1.33	0.06	0.71	0.47	0.02	−0.60	0.40	0.02	−2.40	1.60	0.08
Medial temporalis	1.1	95.6	14	14	−1.37	4.90	−2.94	−0.06	0.01	−0.14	−0.10	0.34	−0.20	−1.42	4.82	−2.83
Post. temporalis	0.7	75.6	12	12	−0.86	2.00	3.56	−0.03	0.06	0.11	−0.04	0.09	0.16	−0.86	2.00	3.52
Inf. lateral pterygoid	1.1	66.9	6	6	0.49	−0.01	0.59	6.74	−1.86	8.11	6.60	1.82	7.90	0.70	−0.08	0.84
Sup. lateral pterygoid	1.0	28.7	4	4	0.44	0.04	0.37	5.35	0.52	4.54	5.13	0.50	4.35	0.55	0.50	0.46

The number of nodes reflects the number of vectors applied to the mandible for each corresponding muscle. The x, y, and z coordinates represent the muscle loads in newtons in each direction. All coordinates are referenced to a global Cartesian coordinate system where the x-y plane is the frontal plane, the x-z represents the horizontal plane, and the y-z indicates the midsagittal plane.

Table 1b Number and Magnitudes of Muscle Loads Used in the Finite Element Model: Maximum Opening and Protrusion

Muscle group	Nodes		Muscle orthogonal components											
			Maximal opening						Protrusion					
			Right			Left			Right			Left		
	Right	Left	x	y	z	x	y	z	x	y	z	x	y	z
Sup. masseter	50	50	−0.34	1.44	0.69	−0.34	1.44	0.69	−0.51	2.14	1.02	−0.51	2.14	1.02
Deep masseter	39	38	−0.15	0.21	−0.10	−0.15	0.21	−0.10	−0.19	0.25	−0.12	−0.19	0.25	−0.14
Medial pterygoid	42	44	0.69	1.12	0.53	0.66	1.07	0.50	1.78	2.90	1.37	1.70	2.77	1.30
Ant. temporalis	20	20	−4.71	3.12	0.01	−4.71	3.12	0.01	−8.06	5.30	0.24	−8.06	5.30	0.24
Medial temporalis	14	14	−0.25	0.91	−0.55	−0.30	1.09	−0.65	−0.05	0.17	−0.10	−0.08	0.28	−0.17
Post. temporalis	12	12	−0.28	0.63	1.13	−0.28	0.63	1.13	−0.05	0.12	0.21	−0.04	0.09	0.14
Inf. lateral pterygoid	6	6	6.30	−1.75	7.60	6.30	−1.75	7.60	6.25	−1.73	7.51	6.25	−1.73	7.51
Sup. lateral pterygoid	4	4	4.26	0.41	3.61	4.15	0.40	3.52	4.64	0.45	3.93	4.64	0.45	3.93

The number of nodes reflects the number of vectors applied to the mandible for each corresponding muscle. The x, y, and z coordinates represent the muscle loads in newtons in each direction. All coordinates are referenced to a global Cartesian coordinate system where the x-y plane is the frontal plane, the x-z represents the horizontal plane, and the y-z indicates the midsagittal plane.

where X_{mi} is the cross-sectional area of muscle mi in cm^2, K is a constant for skeletal muscle (expressed in N/cm^2), and EMG_{mi} is the ratio or scaled value of the muscle contraction relative to its maximum response for a specific task.[17] The product $X_{mi} \cdot K$ is referred to as the weighting factor given to the muscle (Tables 1a and 1b) and EMG_{mi} is considered its scaling factor (Tables 1a and 1b). The product of M_{ir} and its corresponding unit vector yielded the orthogonal vector force components.[17,21] These were subsequently proportioned between the nodes, which formed the corresponding area of muscular attachment (Tables 1a and 1b). The finite element model was loaded with multiple force vectors to simulate muscle forces over wide areas of attachment. Groups of parallel vectors simulated 8 areas of the masticatory muscles (superficial and deep masseter; anterior, middle, and posterior temporalis; inferior, medial, and lateral pterygoid) assumed to be directly attached to bone (Fig 2). Three-dimensional restraints were placed bilaterally at the endosteal surfaces of the temporal bones. These restraints imitated static mandibular movement with fixation of the mandibular apparatus at the cranium. In this way both condyles were assumed to be centered in their glenoid fossae. The model was also restrained only from vertical movement at the alveolar crest (ie, symphysis) anteriorly. Eighteen nodes were not allowed to translate upward. These restraints acted only perpendicularly to the occlusal plane (y-direction), thus allowing free displacement of the mandibular halves, anteroposteriorly, dorso-ventrally, and lateromedially in the horizontal plane.

The implant system and the beams were modeled from predefined solid volumes. The apical part of the implant was in full contact with the lower cortical layer, which is comparable to the clinical situation

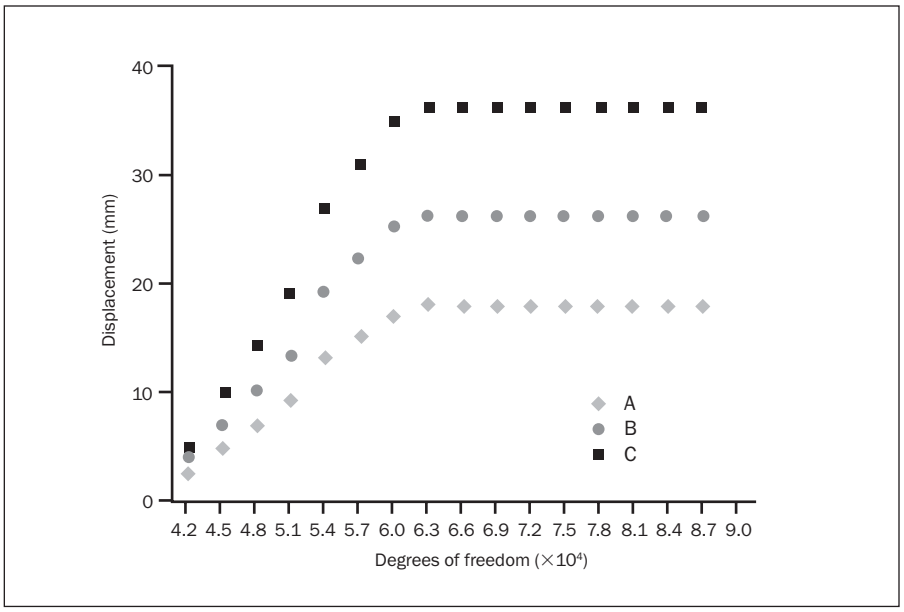

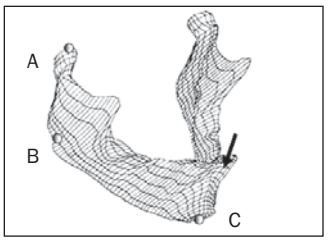

Fig 3 Convergence plots. Displacements of points A, B, and C were plotted against the number of degrees of freedom for the 16 mandibular finite element models (meshes). These 16 models ranged from 14,000 nodes and 42,000 degrees of freedom to 33,341 nodes and 100,023 degrees of freedom. Points A, B, and C correspond to locations where convergence was monitored. The arrow represents the 70-N load used for the convergence test.

(Fig 2). Abutments with a height of 5 mm were modeled connected to the implants. This resulted in a length of 18 mm for the implant-abutment combination. The implant system was assumed to be composed of homogenous and isotropic titanium with a Young's modulus of 103.44 GPa and a Poisson's ratio of 0.35. Since the stress profiles within and about the implant threads were not of interest to this study, it was assumed that the fixation was rigid (ie, there would be no movement between bone and implant under any loading condition).

Any modeling technique is best verified by comparing its results to experimental data. The strain values detected by the measuring transducers were used to verify the modeled jaws as well as to provide empirical values on jaw deformation. In order to establish an accurate finite element model mathematically, more elements and nodes were used until the calculated displacements at a point common to all the meshes approached the exact solution. This is a process known as the *h*-convergence test.[22] Once built, the finite element model was replicated to create 16 finite element models (Fig 3). In all cases, the geometric, material, and boundary conditions were identical. The only difference between these models was in the number of degrees of freedom, with FEM-1 having the fewest degrees of freedom and FEM-16 having the most. To perform the convergence test, a simplified load of 70 N was applied to the midline, while the mandible was loaded with masticatory forces as described. Displacements were calculated at a variety of locations on the mandible.

RESULTS

Jaw Deformation

Predicted and measured data on jaw deformation are presented in Tables 2a and 2b. The strain differences were presented as percentages of the measured values.

Each simulated movement caused the mandible to deform in a different way. Anterolateral views of the finite element model for 1 of the subjects are shown in Fig 4 for maximum opening, right lateral excursions, left lateral excursions, and protrusion. The figure depicts 4 deformed states of the model in which the action of the muscular loads displaced the structural elements, and the model has reached the state of static equilibrium. Displacement has been magnified in the figures to make mandibular deformation more evident. Actual deformations were relatively small; the maximum displacement was 0.8 mm for maximum opening, 1.1 mm for right lateral excursion, 0.9 mm for left lateral excursion, and 1.07 mm for protrusion. During protrusion the jaw deformed in a clockwise manner, and the right side bent upwards and inwards, indicating corporal rotation. During opening the left and right sides of the mandible deformed, turning counterclockwise and clockwise, respectively. During lateral excursions the contralateral side was displaced medially and slightly upwards, rather than being rotated.

Finite Element Model

Convergence Test. The results of the convergence test for calculated displacements at nodes A, B, and C

Table 2a Mean of 5 Measured (M) and Predicted (P) Values of Jaw Deformation for Each Subject: Maximum Opening and Protrusion

	Maximum opening									Protrusion								
	MC			CR			DV			MC			CR			DV		
Subject	M	P	%	M	P	%	M	P	%	M	P	%	M	P	%	M	P	%
1	23.2	24.3	4.7	0.9	1.0	11.0	0.4	0.4	0.0	25.8	27.6	7.0	1.0	1.1	0.1	1.2	1.3	8.3
2	19.3	20.3	5.2	1.6	1.8	12.5	0.9	1.0	11.1	25.8	27.4	6.2	1.6	1.8	12.5	0.8	0.9	12.5
3	41.3	41.9	1.5	2.8	3.0	7.1	1.7	1.8	5.9	56.6	58.4	3.1	2.9	3.0	3.4	1.7	1.9	11.7
4	21.1	22.0	4.3	1.9	2.1	10.5	1.6	1.8	12.5	33.3	36.3	9.0	1.8	1.9	5.6	1.8	1.9	5.6
5	19.4	19.8	2.1	1.8	2.0	11.1	1.8	1.9	5.6	44.4	45.4	0.2	1.8	1.9	5.6	1.6	1.8	12.5
6	14.4	15.4	6.9	2.2	2.5	13.6	1.7	1.9	11.7	28.9	29.5	2.1	2.4	2.6	8.3	1.8	1.9	5.6
7	19.2	20.2	5.2	2.2	2.6	18.2	1.6	1.8	12.5	29.8	29.9	0.3	2.6	2.9	11.5	1.7	1.9	11.7
8	33.4	34.4	3.0	2.0	2.3	15.0	1.8	1.9	5.6	37.4	38.6	3.0	2.0	2.2	10.0	1.8	1.8	0.0
9	50.3	51.3	2.0	1.5	1.7	13.0	1.8	1.9	5.6	55.8	56.9	2.0	1.5	1.8	20.0	1.6	1.8	12.5
10	52.5	53.1	1.1	2.8	3.0	6.6	1.7	1.9	11.7	57.8	58.3	0.1	2.8	2.9	3.5	1.7	1.9	11.7
11	44.2	44.1	0.2	1.9	2.1	10.5	1.2	1.4	16.6	48.2	49.1	1.9	1.9	1.9	0.0	1.8	1.9	5.6
12	33.2	34.2	3.0	1.8	2.2	22.2	1.7	1.9	11.7	39.1	39.8	1.8	1.8	1.9	5.6	1.3	1.5	15.4

Differences between the predicted and measured deformation values were expressed as a percentage of the measured value.

Table 2b Mean of 5 Measured (M) and Predicted (P) Values of Jaw Deformation for Each Subject: Right and Left Lateral Excursions

	Right lateral excursion									Left lateral excursion								
	MC			CR			DV			MC			CR			DV		
Subject	M	P	%	M	P	%	M	P	%	M	P	%	M	P	%	M	P	%
1	11.2	11.3	0.9	2.0	2.2	10.0	1.4	1.6	14.3	17.4	17.6	1.1	1.9	2.0	5.2	1.4	1.6	14.3
2	12.3	12.5	1.6	2.2	2.4	9.0	1.6	1.8	12.5	11.2	11.4	1.8	2.2	2.3	4.5	1.3	1.5	15.3
3	10.3	11.0	6.8	2.2	2.5	13.6	1.8	2.0	11.1	13.4	13.7	2.2	2.1	2.3	9.5	1.6	1.8	12.5
4	14.0	14.5	3.6	2.3	2.5	8.7	1.7	1.9	11.7	11.3	11.6	2.6	2.2	2.4	9.1	1.8	2.0	11.1
5	17.4	17.8	2.3	2.1	2.5	19.0	1.6	1.8	12.5	12.5	12.7	1.6	2.0	2.3	15.0	1.8	2.0	11.1
6	17.4	17.6	1.1	2.3	2.6	11.5	1.8	2.0	11.1	19.2	19.5	1.6	2.2	2.4	9.1	2.0	2.1	5.0
7	11.2	11.6	3.6	2.4	2.6	8.3	1.8	2.0	11.1	11.2	11.5	2.7	2.1	2.4	14.2	1.9	2.0	5.2
8	13.4	15.2	13.4	2.2	2.5	13.6	1.6	1.8	12.5	11.4	11.6	1.8	2.1	2.4	14.2	2.1	2.2	4.8
9	11.3	12.0	6.2	2.0	2.1	10.0	1.5	1.8	0.2	11.2	11.5	2.7	2.0	2.2	10.0	2.6	2.7	3.8
10	12.5	12.8	2.4	2.3	2.5	8.7	1.9	2.1	10.5	12.5	12.7	1.6	2.3	2.4	4.3	1.7	1.8	5.9
11	19.2	19.8	3.1	2.0	2.3	15.0	1.9	2.0	5.2	14.7	14.8	1.0	2.0	2.2	10.0	1.7	1.9	11.8
12	16.2	16.4	1.2	2.0	2.2	10.0	1.1	1.3	18.1	11.8	11.9	1.0	2.0	2.2	10.0	1.8	1.9	5.6

Differences between the predicted and measured deformation values were expressed as a percentage of the measured value.

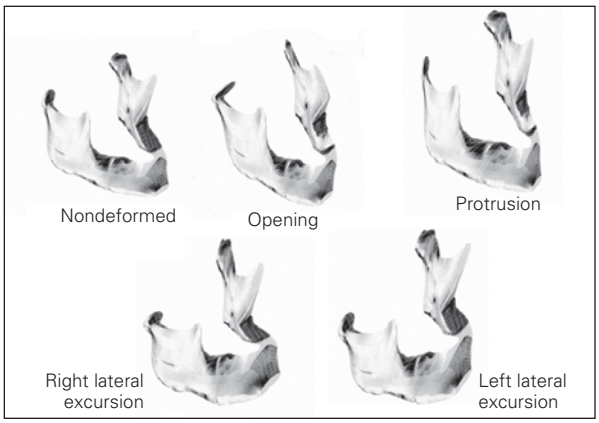

Fig 4 Anterolateral view of the finite element model. Each figure depicts the deformation of the model by the action of the muscular loads displaced on the structural elements. The model shows the state of static equilibrium. Displacement has been magnified in the figures to make mandibular deformation more evident.

were plotted against the number of degrees of freedom in Fig 3, which demonstrates that accurate results were calculated for the nodal displacement with the most refined mesh. Differences in calculated displacements were only 1% to 6% (comparing the results for mesh 8 and mesh 16), whereas the number of degrees of freedom increased by 50% (Fig 4). This indicates that mesh 9 provided accurate results, although only 63,012 degrees of freedom were needed to achieve the convergence.

Stresses. Stress values ranged from 58.2 to 360.2 MPa for the maximum principal stress, from –46.8 to –150.2 MPa for the minimum principal stress, and from 111.3 to 233.3 MPa for the maximum shear stress (Table 3). In all cases the maximum stress occurred either in the subcondylar region, the mandibular angle, or the coronoid notch area, or at the implant level and symphysis (Figs 5 and 6).

Table 3 Maximum Stress Values Predicted by the Finite Element Model

	Jaw position			
Maximum stress (MPa)	Maximum opening	Right lateral excursion	Left lateral excursion	Protrusion
Right side				
Maximum principal	170.2	155.8	58.2	360.2
Minimum principal	−49.4	−46.8	−123.7	−101.1
Maximum shear	133.3	129.2	129.8	233.3
Left side				
Maximum principal	168.6	86.3	162.3	346.3
Minimum principal	−52.1	−150.2	−44.0	−103.3
Maximum shear	129.6	111.3	130.2	215.4

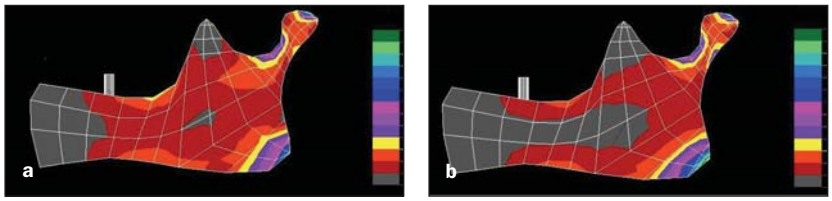

Fig 5 Maximum principal stress bands on the lateral aspect of *(a)* the right and *(b)* left sides of the mandible during protrusion. Colors reflect specific stress magnitudes.

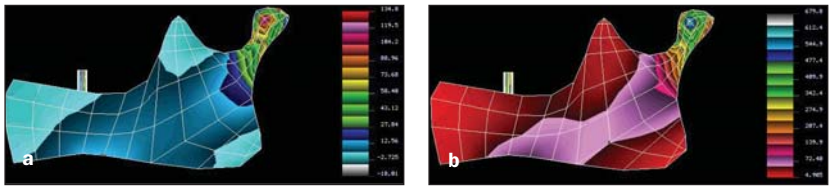

Fig 6 Maximum principal stress bands on the lateral aspect of *(a)* the right and *(b)* left sides of the mandible at maximum opening. Color numbers reflect specific stress magnitudes.

Symphyseal Stress. Special attention was given to analysis of the symphyseal stress analysis because of its role in the deformation of the mandible. Stresses were quantified for maximum opening, protrusion, and right and left lateral excursions at 18 nodes forming the cortical outline of the midsagittal symphyseal region (Fig 7). In all cases, right and left lateral excursion evoked the lowest stress magnitudes. Maximum principal stress was higher on the mandibular border and the anterior (labial) aspect of the symphyseal region than on its posterior (lingual) side during all movements except maximum opening, which evoked higher magnitudes of stress at the posterior aspect of the symphysis. In all cases, the lowest values were found at the most superior and posterior locations. Minimum principal stress had peaks of intensity at the most superior and posterior locations during maximum opening and protrusion. The anterior aspect of the symphyseal region also experienced elevated magnitudes of minimum principal stress during protrusion and maximum opening. The magnitudes of maximum shear stress were distributed approximately symmetrically between the anterior and the posterior aspects of symphyseal region during all movements except for protrusion, which caused higher shear on the anterior symphysis.

DISCUSSION

Finite Element Model

Several 3-dimensional finite element models of the mandible have been created.[23–39] In general, these models have been compromised by the oversimplification of material properties, methods of verification, boundary conditions, and/or mandibular geometry. This present study attempted to answer the following questions: Is the finite element analysis a valid method with which to determine mandibular functional deformations under masticatory muscle loading, clinically? What patterns of deformation can be evaluated during normal mandibular movement?

Verification of the Finite Element Model. Designing the clinical experiment for every subject was a painstaking procedure. Each patient required 3 sets of customized displacement transducers designed to fit within the limits of the available interocclusal distance. Difficulties also arose from the need for tongue space. The deformation of each of the 4 beams could not be measured in isolation, since it has been suggested that all deformation types occurring in the primate mandible take place concurrently.[6] Increasing the sample size would have given more accurate results. However, it might not

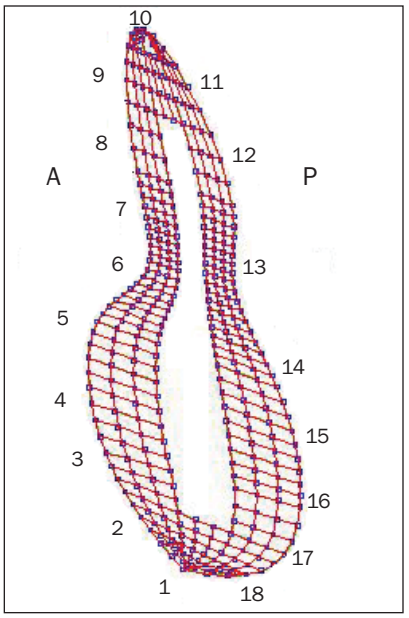

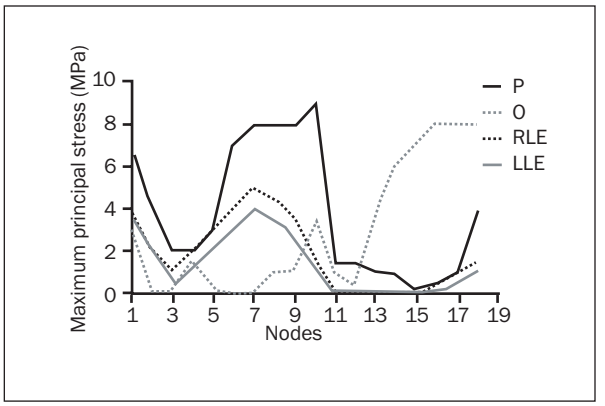

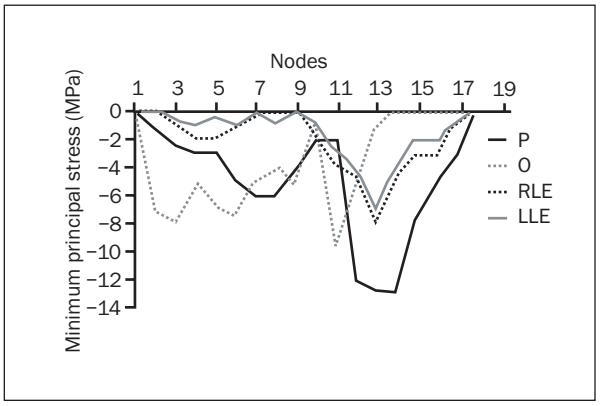

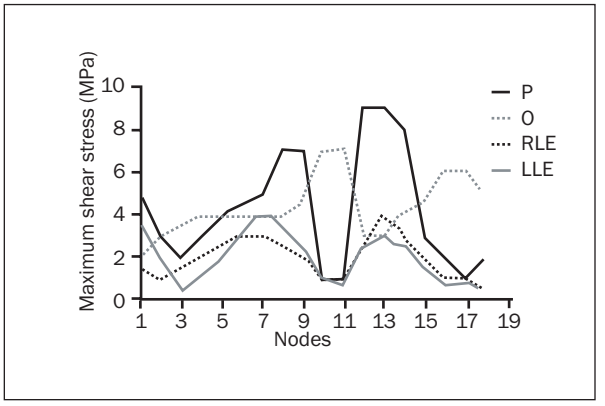

Fig 7 Principal and maximum shear stress magnitudes at the symphysis during various jaw positions. Stress values were plotted at 18 nodes forming the cortical outline of the symphysis. Nodes 2 to 9 were located on the anterior (A) aspect of the symphyseal outline, and nodes 11 to 18 on the posterior (P) side.

have affected the results significantly, since all the subjects were female and of similar age group.

The precision and reliability of a model depends on how well the predicted deformation patterns and values match clinically determined ones. The finite element model was clinically verified through a series of custom-fabricated transducers. In this project, the good agreement between the predicted and measured deformation values indicates the accuracy of the present finite element model. Previous studies have failed to recognize the importance of clinical verification of a finite element model and relied on mathematical validation through an element discretization process.

Few researchers have attempted to make a direct comparison between values predicted by a finite element model and experimental ones on a human mandible.[23,24,33] Gupta et al[23] compared an analytical model with holographic displacement contours and found "good qualitative agreement." Knoell[24] compared strains measured below the teeth on the periosteal surface of cortical bone with values obtained at similar locations in the finite element model. Although he stated that there was reasonable agreement between predicted and test results, this was not the case when the first molar was loaded horizontally.[24] Neither study described the specific method used for comparisons. The same applies to a

large number of finite element analyses in orthopedic research, where the incorrect application of statistical techniques such as correlation and even regression analyses for comparative purposes is common.[22] In many cases, the samples studied (ie, number of models and experimental objects) was inadequate.

Although it is not always technically possible to develop a statistically sufficient number of models owing to the complications inherent in complex modeling techniques, more effort should be made on the validation process, and a more rigorous statistical approach should be adopted. If the objective of the simulation exercise, however, is to find an individual match between a given system and its model—especially when the system under study has a wide variety of possible combinations of parameters—then the application of conventional statistical methods becomes inappropriate. This holds true for the mandibular system, where the comparison between the predicted and measured strain values necessitated the application of alternative statistical approaches, such as comparisons of the means or the goodness-of-fit method. In the case of the former, the statistical method either accepted or rejected the model, which was not satisfactory because of the lack of degree or range of correspondence, which was considered especially important for sensitivity analyses. The goodness-of-fit approach was also rejected, mainly because the actual strains would have been treated incorrectly as observed or expected frequency values, when in fact they were percentages and represented changes in strain values.

The present researchers decided to compare the present data in terms of their percentage differences only, leaving the question of acceptance or rejection open and lending more importance to the increase or decrease in the differences for changes in the model's parameters, as well as to the qualitative comparison between measured and predicted values.

Boundary Conditions

One of the most regular deficiencies of the aforementioned models has probably been the exclusion of biologically relevant boundary conditions, such as the assignment of experimentally derived muscular forces. In the present study, the direction of the putative muscular forces and their line of action were estimated directly from CT scans. However, this was not a simple straightforward procedure, since the masticatory muscles, in particular the human masseter, possess complex pennate anatomy with sophisticated activity patterns. The multiplicity of potential lines of action in the masticatory muscles thus cannot be simply estimated by connecting regression lines through imaged centroids. This may be 1 of the main explanations for the differences between the predicted and measured deformation values.

The aforementioned finite element models included, mainly, the forces caused by teeth in load calculations. This is not necessary because a force produced at the teeth is the resultant of the muscle forces imposed on the mandible and must not be included as an independent factor.

Structural Properties of the Finite Element Model

It would have been ideal to determine the material properties of the mandibular bone used in the present study, since the properties of bone have been shown to vary significantly according to porosity and mineral content,[40] as well as age, gender, and race.[41] It was felt, however, that these factors would not have affected the results significantly, since large variations in material properties (up to 25%) would have been necessary to induce significant changes in the strain patterns.[5,20,21]

Finite element techniques currently used to determine trabecular stress are only able to analyze very small regions of bone with a limited number of trabeculae[42] or a much larger region of bone based on the assumption that it is a solid with apparent material properties.[20,21] In this project, the measurement of the physical properties involved the use of CT to directly derive the mechanical properties of bone.[43] Since a linear relationship exists between the CT number and the apparent density of bone, it is theoretically possible to assess the density of bone from the images and to estimate its elastic modulus using an equation proposed by Carter and Hayes.[44] An alternative approach using ultrasound to determine the mechanical properties of cortical and trabecular bone seems encouraging, since acoustic material testing methods have proved reliable.[23]

In short, the advantages of the model developed in this study are that *(a)* it modeled bone as an orthotropic material, *(b)* it was loaded with experimentally obtained muscular forces, and *(c)* it was clinically verified and mathematically validated.

Jaw Deformation

Medial Convergence. Studies of MC in human subjects during dynamic jaw movements such as opening, retraction, and protrusion have shown that the mandibular dental arch can either widen[45,46] or narrow.[47,48] In the aforementioned experiments, horizontal jaw deformation ranged from 16 to 78 μm and was consistently more pronounced in protrusive movements than in other jaw opening. It may be possible to attribute the wide range of results in the

various investigations to differences in methodology as well as variations in masticatory muscle activity between the subjects tested. The amount of medial convergence measured and predicted in this study fell within the range of the previously published data. MC during opening movements ranged from 14.4 to 53.1 μm. Medial convergence was most extensive in protrusion, ranging between 25.8 and 58.4 μm. The largest value found during protrusion in this study is consistent with other reports and could be attributed to the fact that the onset of lateral pterygoid activity is delayed in jaw opening compared to jaw protrusion.[49] Convergence during lateral movements proved less pronounced (ranging from 10.3 μm to 19.8 μm), similar to data reported by Abdel-Latif[50] and Al-Sukhun and Kelleway.[18] This could be attributed to the fact that during the lateral pterygoids are both active protrusion; during lateral excursion, only one of them is active. The relatively low values of MC found in the present study could also be associated with the fact that the study was carried out on edentulous subjects treated with fixed osseointegrated implants; the transducers were not linked to natural teeth. This study suggests that a more detailed finite element analysis focusing on the bone-implant interface might be of considerable value.

Corporal Rotation. Beecher[51] suggested that CR occurs only during the power stroke of mastication. This study, however, showed that CR occurs immediately on the commencement of movement. The measured and predicted shear angle ranged from 0.9 to 3.0 degrees during opening movements. The range during lateral excursion was smaller (1.9 to 2.6 degrees).

Dorso-ventral Shear. The results show that DV occurs immediately on the commencement of jaw movement, which is in disagreement with Hylander.[6] The results of their study[6] suggested that dorso-ventral shear of the mandible occurred only during unilateral mastication. The shear angle ranged from 0.4 to 1.9 degrees during opening and protrusive movements. The highest value was recorded during protrusion. The range during lateral excursion was narrower and ranged from 1.4 to 2.7 degrees.

Symphyseal Stress as Predicted by the Finite Element Model. During an opening movement, the bilateral rotational corporal deformation was translated mainly into horizontal and frontal bending at the symphysis. The horizontal bending in this study was demonstrated by compressive stress anteriorly and relatively higher tensile stress posteriorly. Bending in the frontal plane was evidenced by high levels of compressive stress in the alveolar crest region and elevated tension at the lower border. Also, evidence in support of lateral bending was demonstrated by compression in the mid-region of the anterior cortical surface of the symphysis and elevated tension on the lingual side. The occurrence of symphyseal bending in the frontal plane in animals during the power stroke of mastication has been suggested,[6] and experimental strain data gathered from the lower anterior (labial) aspect of the macaque symphysis has corroborated its presence.[6–12] Thus, it seems that mandibular movements in humans evoke at least 1 type of symphyseal bending similar to those shown to occur in animals during the power stroke of mastication.

Clinical Significance of Law Deformation

Mandibular deformation is of considerable significance in implant treatment, where the essentially rigid and elastic osseointegrated implant-bone interface, often combined with a rigid superstructure, can be associated with high-stress gradients due to jaw deformation. The possibility that jaw deformation and the resultant stresses may be a source of implant failure, or in some situations enhancement of osseointegration, cannot be excluded.[47,50]

Jaw deformation can be a problem during impression making. An impression taken with the mouth wide open may not fit passively in other jaw positions. Jaw deformation may also be partially responsible for the loosening of implant-supported superstructures when it occurs. The superstructure itself might bend or fracture under stress applied.[47,50]

The long-term clinical significance of jaw deformation in the treatment of conditions such as mandibular fractures, facial deformities, and relapse tendencies following orthognathic surgeries should not be underestimated. The finite element model could be used to determine the most convenient location and design of fracture fixation devices. To specifically test for ideal placement of these devices on the jaw, the finite element model could be used to simulate fractures and the cuts bridged by fixation plates. The model could be used to gather data on areas of stress under different loading conditions and with craniofacial types. The relationship between form and function in the mandibular system could be further explored to include the effects of variations in muscle action on the growth and development of the mandible.

CONCLUSIONS

Based upon this clinically validated finite element model, the following conclusions can be made:

- Close agreement between the predicted and measured deformation values provided a high level of confidence in the finite element model and its ability to provide a better insight into understanding the complex phenomena of functional mandibular deformation.
- Different jaw movements produced different and concurrent patterns of mandibular deformation. Medial convergence ranged between 14.4 and 58.4 μm. Corporal rotation and dorso-ventral shear ranged between 0.4 degrees and 2.7 degrees.
- This study provided stress values of the human jaw when loaded only during normal mandibular movements. Stress values ranged from 58.2 to 360.2 MPa for maximum principal stress, from –46.8 to –150.2 MPa for minimum principal stress, and from 111.3 to 233.3 MPa for maximum shear stress.

ACKNOWLEDGMENTS

The experimental part of the study was undertaken at the Eastman Dental Institute for Oral Health Care Sciences, University of London, United Kingdom. The authors thank the staff of the Prosthetic and Maxillofacial Unit for their wonderful help, support, and friendship.

REFERENCES

1. Wolff J. Das Gesetz der Transformation der Knochen. Berlin: Hirschwald, 1892.
2. Frost HM. Skeletal structural adaptations to mechanical usage (SATMU): 1. Redefining Wolff's law: The bone remodelling problem. Anat Rec 1990;226:403–413.
3. Hylander WL. In-vivo bone strain in the mandible of *Galago crassicaudatus*. Am J Phys Anthrop 1977;46:309–326.
4. Lanyon LE. Functional stress in bone tissue as an objective, and a controlling stimulus for adaptive bone remodelling. J Biomech 1987;20:1083–1093.
5. Al-Sukhun J. Modeling of mandibular functional deformation. London: University of London, 2003:273.
6. Hylander WL. Stress and strain in the mandibular symphysis of primates: A test of competing hypotheses. Am J Phys Anthrop 1984;64:1–46.
7. Hylander WL. The human mandible: Lever or link? Am J Phys Anthrop 1975;43:227–242.
8. Hylander WL. Incisal bite force direction in humans and the functional significance of mammalian mandibular translation. Am J Phys Anthrop 1978;48:1–8.
9. Hylander WL. Mandibular function in *Galago crassicaudatus* and *Macaca fascicularis:* An in-vivo approach to stress analysis of the mandible. J Morphol 1979;159:253–296.
10. Hylander WL. The functional significance of primate mandibular form. J Morphol 1979;160:223–240.
11. Hylander WL, Ravosa MJ, Ross CF, Johnson KR. Mandibular corpus strain in primates: Further evidence for a functional link between symphyseal fusion and jaw-adductor muscle force. Am J Phys Anthrop 1998;107:257–271.
12. Ralph JP, Caputo AA. Analysis of stress patterns in the human mandible. J Dent Res 54:1975;814–821.
13. Mongini F, Calderale PM, Barberi G. Relationship between structure and the stress pattern in the human mandible. J Dent Res 1979;58:2334–2337.
14. Standlee JP, Caputo AA, Ralph JP. The condyle as a stress-distributing component of the temporomandibular joint. J Oral Rehabil 1981;8:391–401.
15. Gysi A. Studies on the leverage problem of the mandible. Dent Digest 1921;27:74–84.
16. Robinson M. The temporomandibular joint: Theory of reflex controlled non-lever action of the mandible. J Am Dent Assoc 1946;33:1260–1271.
17. Korioth TP, Versulis A. Modelling of the biomechanical behaviour of the jaws and their related structures by finite element analysis. Crit Rev Oral Biol Med 1997;8:90–104.
18. Al-Sukhun J, Kelleway J. Biomechanics of the mandible part I: Measurement of mandibular functional deformation using custom-fabricated displacement transducers. J Oral Maxillofac Surg 2006;64:1015–1022.
19. Carter DR, Hayes WC. The compressive behaviour of bone as a two-phase porous structure. J Bone Joint Surg 1977;59:954–962.
20. Al-Sukhun J, Lindqvist C, Kontio R. Modelling of orbital deformation using finite element analysis. J R Soc Interface 2006;3:255–262.
21. Al-Sukhun J, Lindqvist C, Kontio R. Orbital stress analysis. Part II: Variables affecting the predictive behaviour of a finite element model of a human orbit. J Oral Maxillofac Surg (in press).
22. Huiskes R, Hollister SJ. From structure to process, form to organ: Recent developments of FE analysis in orthopaedic biomechanics. J Biomed Eng 1993;115:520–527.
23. Gupta KK, Knoell AC, Grenoble DE. Mathematical modelling and structural analysis of the mandible. Biomat Med Dev Art Org 1973;1:469–479.
24. Knoell AC. A mathematical model of an in-vitro human mandible. J Biomech 1977;10:159–166.
25. Ferré JC, Legoux R, Helary JL, et al. Study of the deformations of the isolated mandible under static constraints by simulation on a physiocomathematical model. Anat Clin 1985;7:183–192.
26. Andersen KL, Mortensen HT, Pedersen EH, Melsen B. Determination of stress levels and profiles in the periodontal ligament by means of an improved three-dimensional finite element model for various types of orthodontic and natural force systems. J Biomed Eng 1999;13:293–303.
27. Hart RT, Hennebel VV, Thongpreda N, Van Buskirk WC, Anderson RC. Modelling the biomechanics of the mandible: A three-dimensional finite element study. J Biomech 1992;25:261–286.
28. Tanne K, Lu Y, Tanaka E, Sakuda M. Biomechanical changes of the mandible from orthopaedic chin cup force studied in a three-dimensional finite element model. Euro J Orthod 1993;15:527–533.

29. Bidez MW, McLoughlin SW, Chen Y, English CE. Finite element analysis of two-abutment Hader bar designs. Implant Dent 1993;2:107–114.
30. van Zyl PP, Grundling NL, Jooste CH, Eugéne T. Three-dimensional finite element model of a human mandible incorporating six osseointegrated implants for stress analysis of mandibular cantilever prosthesis. Int J Oral Maxillofac Surg 1995;10:51–57.
31. Papavasiliou G, Kamposiora P, Bayne S, Felton D. Three-dimensional finite element analysis of stress distribution around single tooth implants as a function of bony support, prosthesis type, and loading during function. J Prosthet Dent 1997;76:633–640.
32. Tiexeira ER, Sato Y, Akagawa Y, Shindoi N. A comparative evaluation of mandibular finite element models with different lengths and elements for implant biomechanics. J Oral Rehab 1998;25:299–303.
33. Vollmer D, Meyer U, Joos U, Vegh A, Piffko J. Experimental and finite element study of a human mandible. J Craniomaxillofac Surg 2000;28:91–96.
34. Gallas Torreira M, Fernandez JR. A three-dimensional computer model of the human mandible in two simulated standard trauma situations. J Craniomaxillofac Surg 2004;5:303–307.
35. Kofod T, Cattaneo PM, Dalstra M, Melsen B. Three-dimensional finite element analysis of the mandible and temporomandibular joint during vertical ramus elongation by distraction osteogenesis. J Craniofac Surg 2005;4:586–593.
36. Vannier MW, Conroy GC, Marsh JL, Knapp RH. Three-dimensional cranial surface reconstructions using high-resolution computed tomography. Am J Phys Anthrop 1985;67:299–311.
37. Sinclair B, Hannam AG, Lowe AA, Wood WW. Complex contour organization for surface reconstruction. Comput Graphics 1989;13:311–319.
38. Nagahara K, Murata S, Nakamura S, Tsuchiya T. Displacement and stress distribution in the temporomandibular joint during clenching. Angle Orthod 1999;69:372–379.
39. Tanaka E, Rodrigod P, Tanaka M, Kawaguchi A, Shibazaki T, Tanne K. Stress analysis in the TMJ during jaw opening by use of a three-dimensional finite element model based on magnetic resonance images. Int J Oral Maxillofac Surg 2001;30:421–430.
40. Currey JD. The effect of porosity and mineral content on the Young's modulus of elasticity of compact bone. J Biomech 1988;21:131–139.
41. Evans FG: Mechanical properties of bone. Springfield, IL: Charles C. Thomas, 1973.
42. Keyak JH, Meagher JM, Skinner HB, Mote CD Jr. Automated three-dimensional finite element modelling of bone: A new method. J Biomed Eng 1990;12:389–397.
43. Vannier MW, Conroy GC, Marsh JL, Knapp RH. Three-dimensional cranial surface reconstructions using high-resolution computed tomography. Am J Phys Anthrop 1985;67:299–311.
44. Ashman RB, Cowin SC, van Buskirk WC, Rice JC. A continuous wave technique for the measurement of the elastic properties of cortical bone. J Biomech 1984;17:349–361.
45. Beecher RM. Functional significance of the mandibular symphysis. Am J Phys Anthrop 1979;159:117–130.
46. Gates GN, Nicholls JI. Evaluation of mandibular arch width change. J Prosthet Dent 1981;46:385–392.
47. Hobkirk JA, Schwab J. Mandibular deformation in subjects with osseointegrated implants. Int J Oral Maxillofac Implants 1991;6:319–328.
48. Horiuchi M, Ichikawa T, Noda M, Matsumoto N. Use of interimplant displacement to measure mandibular distortion during jaw movements in humans. Arch Oral Biol 1997;42:185–188.
49. Ueda R. The activity pattern of the inferior head of lateral pterygoid muscle. J Jpn Prosthet Soc 1992;36:94–107.
50. Abdel-Latif H. Functional Mandibular Deformation in Edentulous Subjects Treated with Dental Implants [thesis]. London: University of London, 1996.
51. Beecher RM. Functional significance of the mandibular symphysis. Am J Phys Anthrop 1979;159:117–130.